Journal of Hazardous Materials 162 (2009) 1025–1033

Contents lists available at ScienceDirect

Journal of Hazardous Materials

journal homepage: www.elsevier.com/locate/jhazmat

Photochemical removal of NO_2 by using 172-nm Xe_2 excimer lamp in N_2 or air at atmospheric pressure

Masaharu Tsuji[a,b,c,*], Masashi Kawahara[b], Kenji Noda[b], Makoto Senda[b], Hiroshi Sako[b], Naohiro Kamo[b], Takashi Kawahara[b], Khairul Sozana Nor Kamarudin[d]

[a] Institute for Materials Chemistry and Engineering, Kyushu University, Kasuga, Fukuoka 816-8580, Japan
[b] Department of Applied Science for Electronics and Materials, Graduate School of Engineering Sciences, Kyushu University, Kasuga, Fukuoka 816-8580, Japan
[c] CREST, Japanese Science and Technology, Nihonbashi, Tokyo 103-0027, Japan
[d] Department of Gas Engineering, Faculty of Chemical and Natural Resources Engineering, Universiti Teknologi Malaysia, 81310 UTM Skudai, Malaysia

ARTICLE INFO

Article history:
Received 28 January 2008
Received in revised form 27 April 2008
Accepted 27 May 2008
Available online 9 July 2008

Keywords:
deNOx
VUV photolysis
Excimer lamp
Ozone Environmental technology

ABSTRACT

Photochemical removal of NO_2 in N_2 or air (5–20% O_2) mixtures was studied by using 172-nm Xe_2 excimer lamps to develop a new simple photochemical aftertreatment technique of NO_2 in air at atmospheric pressure without using any catalysts. When a high power lamp (300 mW/cm^2) was used, the conversion of NO_2 (200–1000 ppm) to N_2 and O_2 in N_2 was >93% after 1 min irradiation, whereas that to N_2O_5, HNO_3, N_2, and O_2 in air (10% O_2) was 100% after 5 s irradiation in a batch system. In a flow system, about 92% of NO_2 (200 ppm) in N_2 was converted to N_2 and O_2, whereas NO_2 (200–400 ppm) in air (20% O_2) could be completely converted to N_2O_5, HNO_3, N_2, and O_2 at a flow rate of 1 l/min. It was found that NO could also be decomposed to N_2 and O_2 under 172-nm irradiation, though the removal rate is slower than that of NO_2 by a factor of 3.8. A simple model analysis assuming a consecutive reaction $NO_2 \rightarrow NO \rightarrow N + O$ indicated that 86% of NO_2 is decomposed directly into $N + O_2$ and the rest is dissociated into $NO + O$ under 172-nm irradiation. These results led us to conclude that the present technique is a new promising catalyst-free photochemical aftertreatment method of NO_2 in N_2 and air in a flow system.

© 2008 Elsevier B.V. All rights reserved.

1. Introduction

Nitrogen oxides (NOx: NO and NO_2), which arise from various industrial sources, are major contributors to the acid rain [1,2]. Removal methods of NOx by using catalysts have been extensively studied and widely applied as aftertreatment techniques in automobiles and thermal power plants [3–5]. Catalysts must be not only active at low reaction temperatures in the presence of components such as O_2, CO, CO_2, H_2O, and hydrocarbons usually present in the exhausted gases, but also resistant to deactivation by SO_2. Selective catalytic reduction (SCR) is widely applied as a cleaning method of fuel gas. Removal processes of NOx are as follows:

$$4NO + 4NH_3 + O_2 \rightarrow 4N_2 + 6H_2O \quad (1a)$$

$$6NO_2 + 8NH_3 \rightarrow 7N_2 + 12H_2O \quad (1b)$$

Non-selective catalytic reduction (NSCR) needs injection of NH_3 or other reducing agents without catalysts. The deNOx reaction is as follows:

$$CO(NH_2)_2 + 2NO + 1/2O_2 \rightarrow 2N_2 + CO_2 + 2H_2O \quad (2)$$

In the above SCR and NSCR processes, such expensive reducing agents as NH_3 and $CO(NH_2)_2$ are required and global warming CO_2 gas is emitted in the NSCR process (2).

Removal of NOx was also studied by using pulsed corona discharge [6–13] and microwave discharge methods [14–23]. Discharge methods will become a low cost convenient method, if NOx can be removed without using any catalysts and reducing agents. In our previous study using microwave discharge, NO could be efficiently decomposed into N_2 and O_2 in N_2 at atmospheric pressure [19]. In most of the exhausted gases containing NOx, O_2 less than 20% is usually involved. In such cases, it is generally very difficult to completely suppress NOx emission resulting from plasma discharge of buffer N_2/O_2 gases without using catalysts. Recently, costs of rare metal catalysts increase greatly because of economic growth of developing countries. Therefore, a new low-cost and catalysts-free aftertreatment process in air must be developed to overcome this problem.

The reason why discharge processes are difficult to remove NOx is that dominant energy carrier in electric discharges is energetic

* Corresponding author at: Institute for Materials Chemistry and Engineering, Kyushu University, Kasuga, Fukuoka 816-8580, Japan. Fax: +81 92 583 7815.
E-mail address: tsuji@cm.kyushu-u.ac.jp (M. Tsuji).

0304-3894/$ – see front matter © 2008 Elsevier B.V. All rights reserved.
doi:10.1016/j.jhazmat.2008.05.136

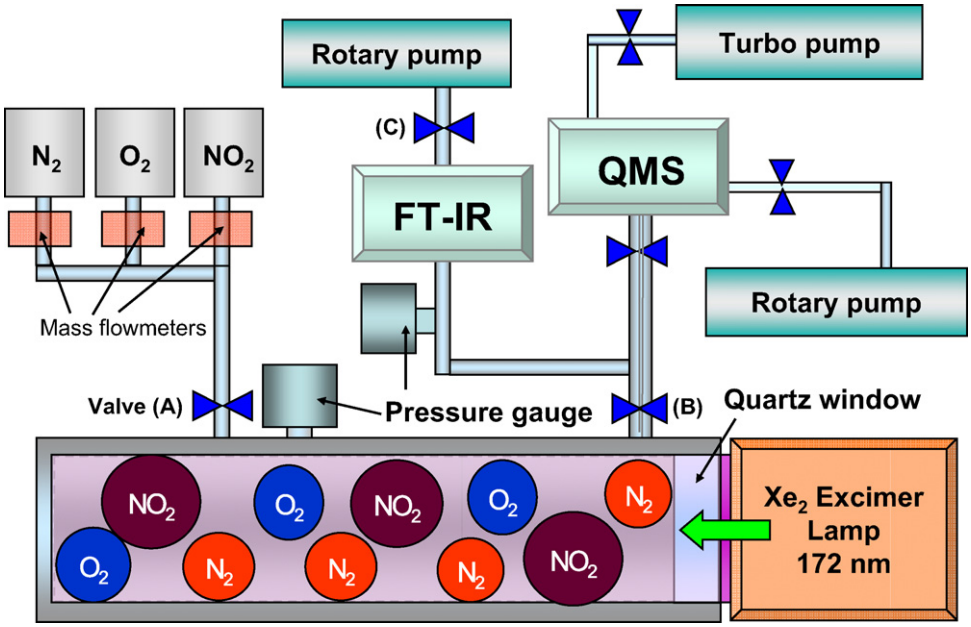

Fig. 1. deNOx apparatus using a Xe_2 excimer lamp.

electrons. The disadvantage of discharge processes arises from a low selectivity of gas phase reactions of energetic electrons with NOx and buffer N_2/O_2 gases. In an electric discharge of NOx in air, electron-impact excitation, ionization, and dissociation of NOx, N_2, and O_2 occur simultaneously and subsequent various secondary reactions lead to NOx emission. Thus, a higher selectivity in gas phase reactions is required in order to remove NOx efficiently in air.

We have recently initiated a systematic study on photochemical removal of NOx at atmospheric pressure in air [24–28]. An advantage of photochemical method is that more selective decomposition is possible than that in electric-discharge methods, because there are large differences in the absorption coefficients of gas components in exhausted gases. N_2 has no absorption in the 170–200 nm region, although it is easily decomposed and ionized in electric discharges by impact of accelerated electrons. If N_2, which is a major component in most of exhausted gases, is inert, reactions in the systems become simple and decomposition efficiencies of NOx are expected to increase greatly.

By using this high selectivity in photoabsorption in the vacuum ultraviolet (VUV) region, we have recently attempted photochemical removal of NO_2 at atmospheric pressure by using a 193-nm ArF excimer laser [25] and a low-power (50 mW/cm^2) 172-nm Xe_2 excimer lamp [28]. The former photon source was a high power pulse laser with a pulse width of about 25 ns, whereas the latter one was a continuous wave (CW) lamp. The advantages of the latter excimer lamp in comparison with that of the former excimer laser are compact size, low price, low running cost, and poisonous F_2 gas free.

When 193-nm ArF excimer laser was used, more than 80% of NO_2 (200 ppm) could be converted into N_2, O_2, and NO in N_2 at atmospheric pressure. However, it was difficult to decompose NO_2 in air because after photolysis of NO_2 into NO + O (3), such backward reactions (4)–(6) occur significantly [1,25,28–31]:

$$NO_2 + h\nu(193\,\text{nm}) \rightarrow NO + O\,(7.1 \times 10^{-19}\,\text{cm}^2\,\text{molecule}^{-1}) \quad (3)$$

$$NO + O + M \rightarrow NO_2 + M\,(1.0 \times 10^{-31}\,\text{cm}^6\,\text{molecule}^{-2}\,\text{s}^{-1}\ \text{for M} = N_2) \quad (4)$$

$$2NO + O_2 \rightarrow 2NO_2\,(1.93 \times 10^{-38}\,\text{cm}^6\,\text{molecule}^{-2}\,\text{s}^{-1}) \quad (5)$$

$$NO + O_3 \rightarrow NO_2 + O_2\,(1.8 \times 10^{-14}\,\text{cm}^3\,\text{molecule}^{-1}\,\text{s}^{-1}) \quad (6)$$

The absorption cross section of NO_2 at 172 nm is about 20 times larger than that at 193 nm [31]:

$$NO_2 + h\nu(172\,\text{nm}) \rightarrow \text{Products}\,(1.4 \times 10^{-17}\,\text{cm}^2\,\text{molecule}^{-1}) \quad (7)$$

The dissociation energy of NO (6.50 eV) is higher than the photon energy of 193-nm light (6.42 eV), whereas it is lower than that of 172-nm light (7.21 eV) [31,32]:

$$NO + h\nu(193\,\text{nm}) \rightarrow N(^4S) + O(^3P) - 0.08\,\text{eV} \quad (8a)$$

$$NO + h\nu(172\,\text{nm}) \rightarrow N(^4S) + O(^3P) + 0.71\,\text{eV} \quad (8b)$$

Therefore, NO can be energetically decomposed into N + O under 172-nm irradiation. We have recently studied photolysis of NO_2 by using a low power 172-nm Xe_2 excimer lamp (50 mW/cm^2) [28]. It was found that the NO_2 conversion in N_2 was 99% and the formation ratios of N_2, O_2, NO, and N_2O were 47, 98, 0, and 2%, respectively, after 30 min irradiation. The NO_2 in air (5–20% O_2) could be efficiently converted to N_2O_5 and HNO_3 due to reactions by O_3 and H_2O (impurity) after only 1.0–1.5 min irradiation. All of the above experiments were carried out in a closed batch system. However, a continuous flow system is required for the practical use of the photochemical NOx removal system. When we attempted to decompose NOx in a flow system by using the ArF excimer laser and the low-power Xe_2 excimer lamp, it was difficult to remove NOx probably due to slow removal rates. In the present study, we have used not only the low-power lamp (50 mW/cm^2) but also a high-power (300 mW/cm^2) Xe_2 lamp. Then, it was found that NO_2 (200–400 ppm) can be removed completely in air in a flow system. Possible photochemical processes are discussed using known photochemical and gas phase reactions [29–31].

2. Apparatus

Fig. 1 shows a deNOx chamber having an inside volume of 185 cm^3 used in this study. Light from an unfocused 172-nm Xe_2 lamp (USHIO, UER20H172: 50 or 300 mW/cm^2, 155–200 nm range) was used to remove NOx at a room temperature. The low-power

Xe_2 lamp was a commercial product, whereas the high-power one was a trial product of USHIO Inc. The size of a low-power Xe_2 lamp (50 mW/cm^2) was ϕ = 30 mm and length = 200 mm, whereas that of a high-power Xe_2 lamp (300 mW/cm^2) was ϕ = 70 mm and length = 240 mm.

Experiments were carried out not only in a closed batch system used in the previous study [28] but also in a flow system. The total pressure was kept at atmospheric pressure and the NO_2 or NO concentration diluted in pure N_2 or air (5–20% O_2) was 200–1000 ppm (v/v). In the batch system, desired gas mixtures were introduced through mass flow controllers and valves (A) and (B) in Fig. 1 were closed. Then, the lamp was irradiated from the right side. In the flow system, stop valves (A)–(C) were open during experiments and the flow rates of each gas were controlled by mass flow controllers. It was kept at 1 l/min in the present experiments. The total pressure was controlled by using valve (B).

In the batch experiments, before and after photo-irradiation, outlet gases were analyzed by using HORIBA gas analysis system (FG122-LS) equipped with an FTIR spectrometer and ANELVA gas analysis system (M-200GA-DTS) equipped with a quadrupole mass spectrometer. On the other hand, outlet gases were analyzed on line by using the FTIR spectrometer in the flow experiments. The low sensitive mass spectrometer was used for the determination of N_2/O_2 ratios of buffer gases, whereas the high sensitive FTIR system was used for the detection of NOx and O_3. The light path length and volume of analyzing chamber in FTIR was 2.4 m and 300 cm^3, respectively. The spectra were measured in the 900–5000 cm^{-1} region with an optical resolution of 4 cm^{-1}. The reliable calibration curves of NOx (NO, NO_2, and N_2O) in FTIR measurements were supplied by HORIBA Inc. The detection limits of NO_2, NO, and N_2O were, 1, 1, and ~0.5 ppm, respectively, in our FTIR spectrometers. The concentrations of N_2O_5, HNO_3, and O_3 were evaluated by reference to their standard spectral data supplied by HORIBA Inc. The experimental accuracies in the measurements of concentrations of NOx and O_3 were ±3%. We determined the residual amount of NOx, $[NOx]/[NOx]_0$, and the formation ratios of N_2, O_2, N_2O_5, and HNO_3 defined as $[N_2]/[NOx]_0$, $[O_2]/[NOx]_0$, $[N_2O_5]/[NOx]_0$, and $[HNO_3]/[NOx]_0$, respectively, from gas analyses. Here, $[NOx]_0$ is an initial concentration of NOx. N_2 and O_2 cannot be detected by FTIR, because these diatomic molecules are inactive for IR light. If other NOx such as N_2O and N_2O_5 and O_3 are produced in the photolysis, all of them can be detected. Thus, the formation ratios of N_2 and O_2 in N_2 were determined from N and O balance before and after photolysis resprctively.

The following gases were used without further purification: N_2 (Taiyo Nissan Inc.: purity >99.9998%), O_2 (Nippon Sanso Inc.: purity >99.99995%), NO_2 (Nippon Sanso Inc.: 3630 ppm in high purity N_2), NO (Taiyo Sanso Inc.: 2.02% in high purity N_2), and N_2O (Nippon Sanso Inc.: 959 ppm in high purity). NO_2 and NO were diluted in N_2 or N_2/O_2 mixtures before use.

3. Results and discussion

3.1. NO_2 removal in N_2 in a batch system

At first, the decomposition of NO_2 in N_2 was studied by using low-power (50 mW/cm^2) and high-power (300 mW/cm^2) lamps in a closed batch system. When the low-power lamp was used, besides NO_2 bands at about 1630 and 2920 cm^{-1}, a weak NO band appeared around 1840 cm^{-1} after 172-nm irradiation. This indicates that the following reaction pathway is open:

$$NO_2 + h\nu\,(172\,\text{nm}) \rightarrow NO + O \quad (9)$$

On the other hand, no NO band was observed by using the high-power lamp. On the basis of this fact, it is reasonable to assume that NO formed through process (9) can efficiently be converted to N_2 and O_2 at the high power probably due to subsequent photolysis of NO (10) and secondary reactions (11)–(13) [29–31]:

$$NO + h\nu\,(172\,\text{nm}) \rightarrow N + O \quad (10)$$

$$2N + M \rightarrow N_2 + M\,(4.82 \times 10^{-33}\,\text{cm}^6\,\text{molecule}^{-2}\,\text{s}^{-1}\,\text{for M} = N_2) \quad (11)$$

$$2O + M \rightarrow O_2 + M\,(8.91 \times 10^{-33}\,\text{cm}^6\,\text{molecule}^{-2}\,\text{s}^{-1}\,\text{for M} = N_2) \quad (12)$$

$$N(^4S) + NO \rightarrow N_2 + O(^3P)\,(2.92 \times 10^{-11}\,\text{cm}^3\,\text{molecule}^{-1}\,\text{s}^{-1}) \quad (13)$$

Fig. 2a and b shows the dependence of residual amount of NO_2 and the formation ratios of NO, N_2O, N_2, and O_2 on the irradiation time of lamp in N_2 obtained by using the two lamps at an initial NO_2 concentration of 1000 ppm. When the low-power lamp was used, the residual amount of NO_2 decreases to 25% after 5 min and slowly decreases to 7% after 30 min photo-irradiation, whereas the formation ratio of N_2 and O_2 increases to 46 and 93%, respectively. The formation ratio of NO initially increases to 6% until 5 min then gradually decreases to 0% in the 5–20 min range. The formation ratio of N_2O was less than 1% in the all time range. When the high-power lamp was used, decomposition rate of NO_2 increases significantly and the formation of NO and N_2O was not observed. The residual amount of NO_2 rapidly decreases to 7% after 1 min irradiation and slowly decreases to zero in the 1–30 min range. There are small parts like a vacuum gauge, which got little VUV light in the photolysis chamber. This may be one reason for the slow decrease in the residual amount of NO_2 in the 1–30 min range, though a further experiment is necessary to conclude the validity of this explanation. The formation ratios of N_2 and O_2 increase rapidly to 46 and 93% at 1 min and become 50 and 100% after 30 min irradiation. On the basis of these results, NO_2 can be efficiently decomposed to N_2 and O_2 in N_2 at 1 atm keeping NO and N_2O emissions at low levels under 172-nm irradiation.

3.2. NO removal in N_2 in a batch system

In order to confirm the contributions of processes (10)–(13), the photolysis of NO under 172-nm irradiation was also studied. Fig. 3a and b shows the dependence of residual amount of NO and the formation ratios of NO_2, N_2O, N_2, and O_2 on the irradiation time in N_2 obtained by using the two lamps at an initial NO concentration of 1000 ppm. When the low-power lamp was used, the residual amount of NO decreases to 59 and 37% after 5 and 10 min irradiation, whereas the formation ratio of NO_2 increases to 10% in the 0–10 min range and slowly decreases to 4% in the 10–30 min range. The formation of a small amount of N_2O less than 2% was observed in the all time range. When the high-power lamp was used, the decomposition rate of NO increases significantly. The residual amount of NO rapidly decreases to 6% after 5 min irradiation and slowly decreases to zero in the 5–20 min range. Although N_2O was not produced, NO_2 was observed in the short time range below about 5 min. Its formation ratio has a peak (~10%) at 1 min. The formation ratios of N_2 and O_2 increase rapidly to 46 and 47% at 5 min and become ~50% after 30 min irradiation. On the basis of these results, NO can be efficiently decomposed to N_2 and O_2 in N_2 keeping NO_2 and N_2O emissions at low levels under 172-nm irradiation.

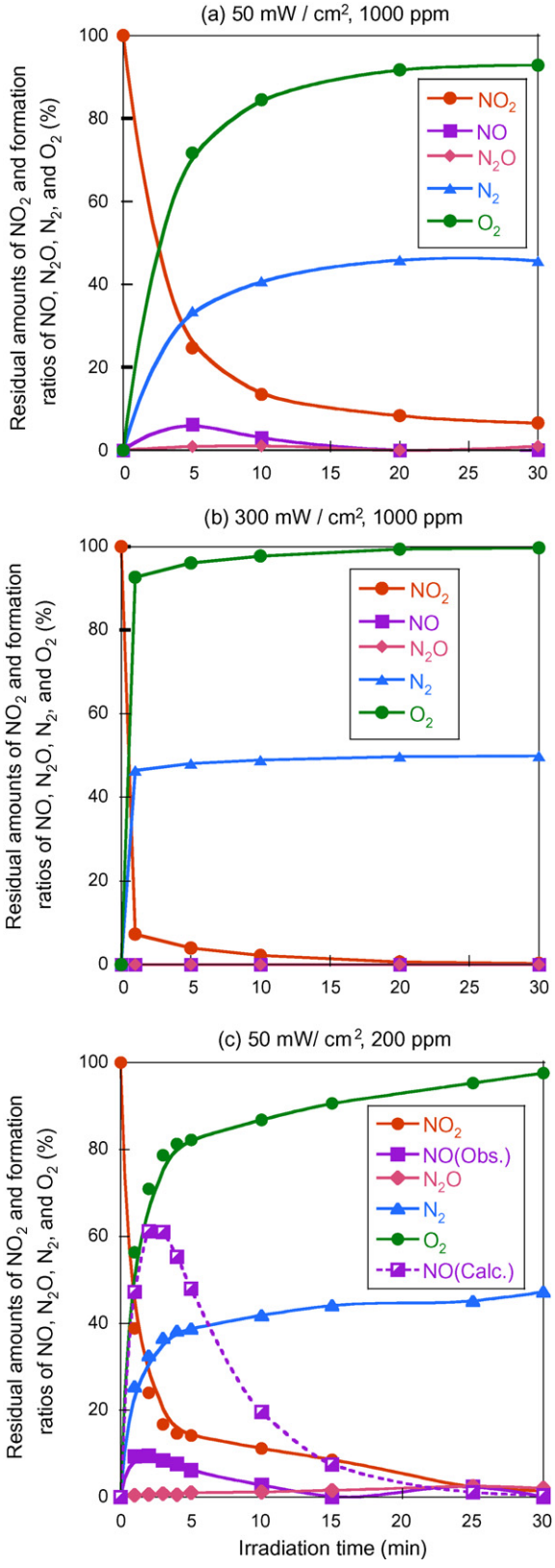

Fig. 2. Dependence of the residual amount of NO_2 and the formation ratios of NO_2, NO, N_2O, N_2, and O_2 on the irradiation time in N_2.

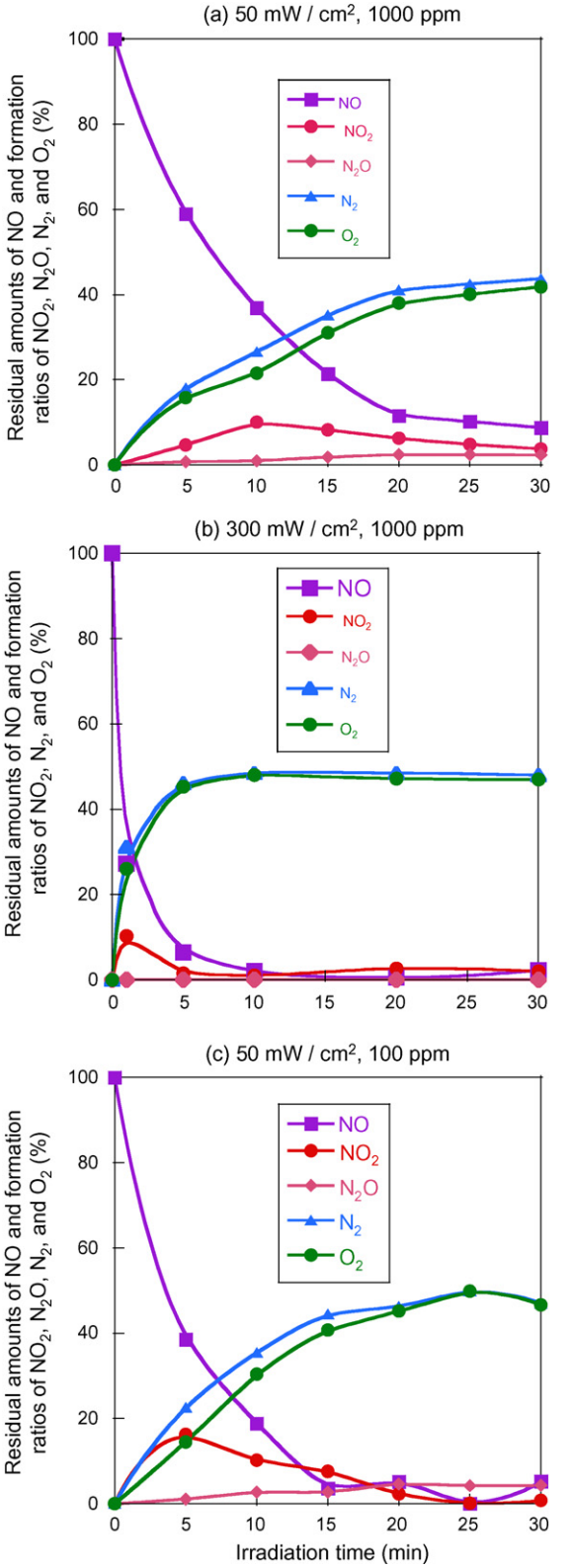

Fig. 3. Dependence of the residual amount of NO and the formation ratios of NO_2, N_2O, N_2, and O_2 on the irradiation time in N_2.

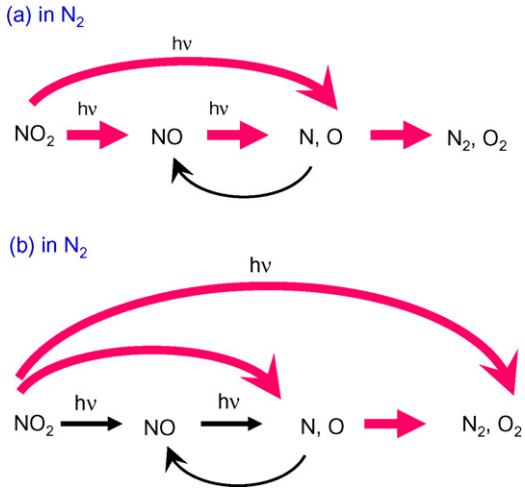

Fig. 4. Two typical models of major decomposition processes of NO_2 in N_2 under 172-nm irradiation.

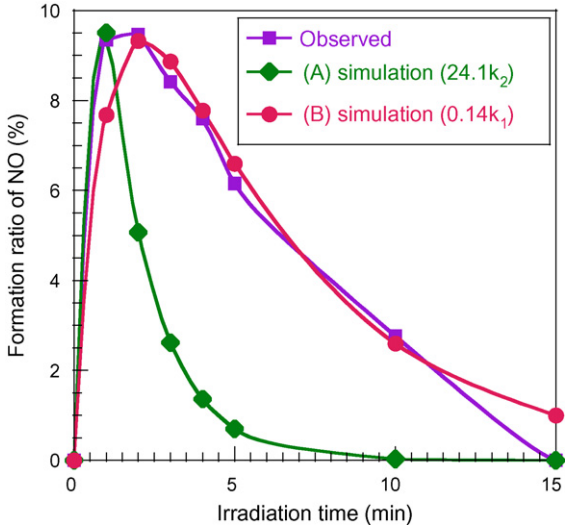

Fig. 5. Dependence of the residual amount of NO_2 and the formation ratio of NO on the irradiation time in N_2 obtained by experiment and consecutive reaction models using various rate constants.

3.3. Mechanism of NO_2 removal in N_2 in a batch system

The reaction mechanism of NO_2 in N_2 under 172-nm irradiation is discussed from known photochemical and chemical reactions [29–31]. We found here that NO_2 is efficiently decomposed into N_2 and O_2 under 172-nm light in N_2 atmosphere keeping the formation ratios of NO and N_2O at low levels (<10%). Although the total absorption coefficient of NO_2 at 172 nm is known [31], little information on their products and yields has been reported to the best of our knowledge. However, kinetic analysis of the time profile of NO concentration provides useful information on the photolysis of NO_2 under 172-nm irradiation.

Two reaction models were considered here for the photolysis of NO_2 under 172-nm irradiation. Fig. 4a shows the first model as major decomposition processes of NO_2 in N_2, where major pathways are shown by bold red lines and minor pathways are given by thin black lines. NO_2 is initially dissociated into NO + O. Then, the product NO is dissociated into N + O. The three-body recombination reactions of 2N + M and 2O + M led to N_2 and O_2, which are major final products. When NO is produced from the three-body reaction N + O + M, NO is produced again. The relative contribution of the N + O + M reaction to those of 2N + M and 2O + M reactions becomes small with increasing the reaction time, because NO concentration decreases with increasing the reaction time. Then, it is finally converted to N_2 and O_2 at a long irradiation time.

The most important finding in the present study is that no NO is produced by using the high-power lamp. In our separate experiment using pure NO (see Section 3.2), we found that the conversion of NO into N_2 and O_2 really occurs under 172-nm photolysis. The removal rates of NO_2 and NO under 172-nm irradiation were determined assuming that they obey the following simple first order decay of molecules:

$$[NO_2] = [NO_2]_0 \exp(-k_1 t) \quad (14a)$$

$$[NO] = [NO]_0 \exp(-k_2 t) \quad (14b)$$

The k_1 value was estimated to be $1.10 \times 10^{-2}\ s^{-1}$ by using removal data at a low NO_2 concentration of 200 ppm (Fig. 2c), where secondary reactions were expected to be reduced than those at 1000 ppm. In this concentration, a small amount of NO (<20 ppm) is produced. It was difficult to estimate a reliable removal rate of NO under such a low concentration in our FTIR spectrometer, the removal rate of NO was determined by using data at 100 ppm (Fig. 3c). It was $2.86 \times 10^{-3}\ s^{-1}$, which is smaller than that of NO_2 by a factor of 3.8. We estimated these k_1 and k_2 values from linear first order decay plots. The correlation kinetic coefficients (R2) of k_1 and k_2 values in the linear plots were 0.928 and 0.941, respectively. It is therefore reasonable to assume that removal rates of NO_2 and NO under 172-nm obey the simple first order.

Assuming a simple consecutive reaction in the 172-nm photolysis of NO_2:

$$NO_2 \xrightarrow{k_1} NO \xrightarrow{k_2} N + O \quad (15)$$

the concentrations of NO_2 and NO under the low-power lamp irradiation were calculated as a function of irradiation time using above k_1 and k_2 values. In the consecutive reaction (15), since the rate-determining step is the secondary photolysis of NO, NO will be observed as a major product. The calculated NO concentrations after photo-irradiation are shown in Fig. 2c (broken line) together with the experimental data for comparison. It should be noted that the maximum NO concentration at 2 min predicted from model calculations is higher than the observed one by a factor of 6.5. On the basis of these facts, the experimental data cannot be reproduced from the above simple consecutive reaction. There are two possible reasons for the explanation of this discrepancy between model (a) and experimental data.

One possible reason is the contribution of vibrationally excited states of NO produced through the $NO_2 + h\nu(172\ nm) \rightarrow NO^* + O$ photolysis. Unfortunately, no data on the initial vibrational distributions of $NO(X^2\Pi : v'')$ under 172-nm irradiation has been reported. However, it is known that vibrationally excited $NO(X^2\Pi : v'' \leq 14)$ levels are initially produced after 193-nm ArF laser photolysis of NO_2 [33,34]. Since the excitation energy of 172 nm (7.21 eV) is much higher than that of 193 nm (6.42 eV), product $NO(X:v'')$ molecules will be more vibrationally excited. If such vibrationally excited levels absorb 172-nm light again, NO will be excited into higher excited states, from which predissociation to N + O atoms occurs more rapidly than that produced from the $NO(X:v'' = 0)$ level. When k_2 values were changed to reproduce experimental data, the best fit k_2 value for the peak value was $6.89 \times 10^{-2}\ s^{-1}$, as shown in Fig. 5 (case (A)). This value was 24.1 times larger than the observed k_2 value. No reasonable agreement between observed and calculated values was obtained because the calculated value decreases more rapidly than the observed one after about 1 min.

It is known that vibrationally relaxation is fast for excited states of NO(X:$v'' > 0$) by collisions with NO_2 [33–35]. Thus, at high NO_2 concentration, vibrational relaxation by collisions with NO_2 becomes significant. In such a case, excitation into high-energy predissociation states will be suppressed and the product distribution reflects simple photolysis of NO(X:$v'' = 0$) into N + O expressed by the measured k_2 value. If vibrational relaxation by collisions with NO_2 becomes insignificant, NO concentration will decrease with decreasing NO_2 concentration. Fig. 2c shows the experimental data at a low NO_2 concentration of 200 ppm. The maximum formation ratio of NO at 200 ppm is about 9% at 1–2 min, which is higher than that at 1000 ppm (6%). On the basis of this fact, it was concluded that the contribution of vibrationally excited NO* was insignificant under the present experimental conditions.

The other possible reason is a direct pathway leading to N + O_2 besides NO + O pathway:

$$NO_2 + h\nu\ (172\,\text{nm}) \xrightarrow{k_{1a}} NO + O(^3P,\ ^1D,\ ^1S) \quad (16a)$$

$$NO_2 + h\nu\ (172\,\text{nm}) \xrightarrow{k_{1b}} N + O_2 \quad (16b)$$

Here, the following relation $k_1 = k_{1a} + k_{1b}$ holds. In this case the concentration of NO is given by

$$[NO] = \frac{k_{1a}}{\{k_2 - (k_{1a} + k_{1b})\}} [\exp\{-(k_{1a} + k_{1b})t\} - \exp(-k_2 t)][NO_2]_0 \quad (17)$$

When various k_{1a} and k_{1b} values are used to reproduce the experimental data, the best-fit curve was obtained at $k_{1a} = 1.8 \times 10^{-3}\ s^{-1}$ and $k_{1b} = 1.08 \times 10^{-2}\ s^{-1}$, as shown in Fig. 5 (case (B)). Therefore, the branching ratios of (16a) and (16b) were estimated to be 14 and 86%, respectively. This shows that the direct formation process of O_2 is faster than that of NO by a factor of 6. Thus, the revised second decomposition model (b) is shown in Fig. 4b, where the direct photolysis of NO_2 to N + O_2 is significant.

3.4. NO_2 removal in air in a batch system

Since small amounts of O_2 (5–20%) are involved in N_2/O_2 mixtures in the practical fuel combustion gases, removal techniques of NO_2 must be developed in air. The most outstanding difference between 172-nm irradiation and 193-nm one in air is that the absorption coefficient of O_2 at 172 nm ($4.6 \times 10^{-19}\ cm^2\ molecule^{-1}$) is 1440 times larger than that at 193 nm ($3.2 \times 10^{-22}\ cm^2\ molecule^{-1}$) [31]. Thus, higher concentrations of O_3 are produced in the reaction system in the presence of O_2.

Fig. 6a and b shows FTIR spectra observed before and after 172-nm photolysis of NO_2 (200 ppm) in air (O_2 5%) using the low-power lamp. Before photolysis, strong NO_2 peak is observed. After 1 min photo-irradiation, the spectrum changed significantly, and NO_2 peak disappeared and N_2O_5, HNO_3, and O_3 peaks are observed. We have measured the dependence of residual amount of NO_2 and the formation ratios of products on the irradiation time of lamp at various O_2 concentrations in the 5–20% range. As a typical example, Fig. 7a and b shows results obtained in air (O_2 5%) by using the two lamps at an initial NO_2 concentration of 200 ppm. NO_2 can be efficiently converted to N_2O_5 and HNO_3 in the presence of O_2 due to the efficient formation of O_3 by photolysis of O_2 under 172-nm irradiation. At the NO_2 concentration of 200 ppm, NO_2 can be removed after about 1 min by using the low-power lamp and only 5 s by using the high-power lamp.

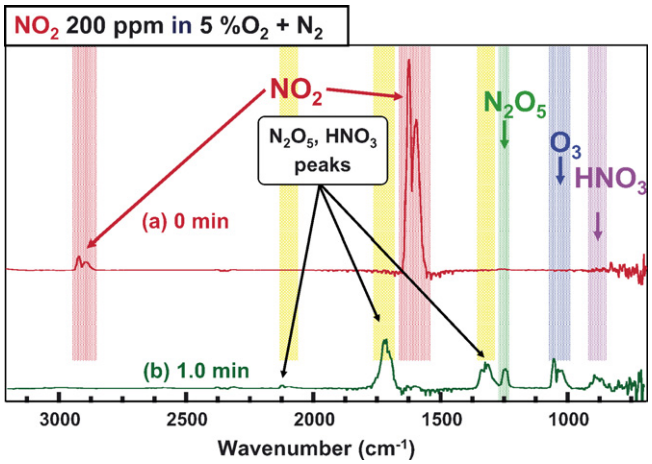

Fig. 6. FTIR spectra of NO_2 in air (5% O_2) under 172-nm irradiation observed at 0 and 1.0 min. The initial NO_2 concentration was 200 ppm.

3.5. NO_2 removal in N_2 and air in a flow system

For the actual application of photochemical removal of exhausted gases, a flow system, in which continuous removal of exhausted gases is possible, is required. We found that it was diffi-

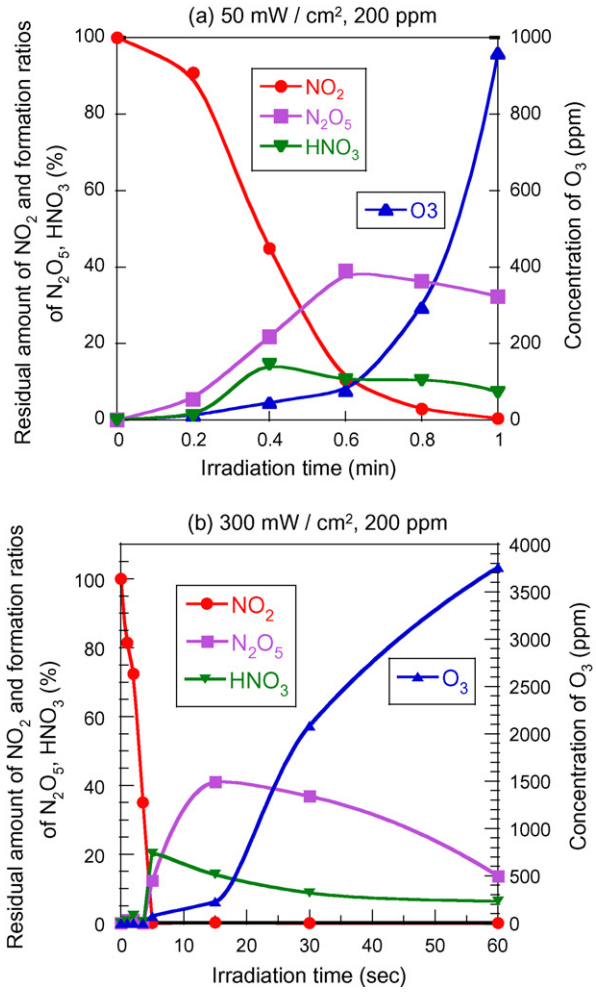

Fig. 7. Dependence of residual amount of NO_2 and the formation ratios of products on the irradiation time in air (5% O_2). The initial NO_2 concentration was 200 ppm.

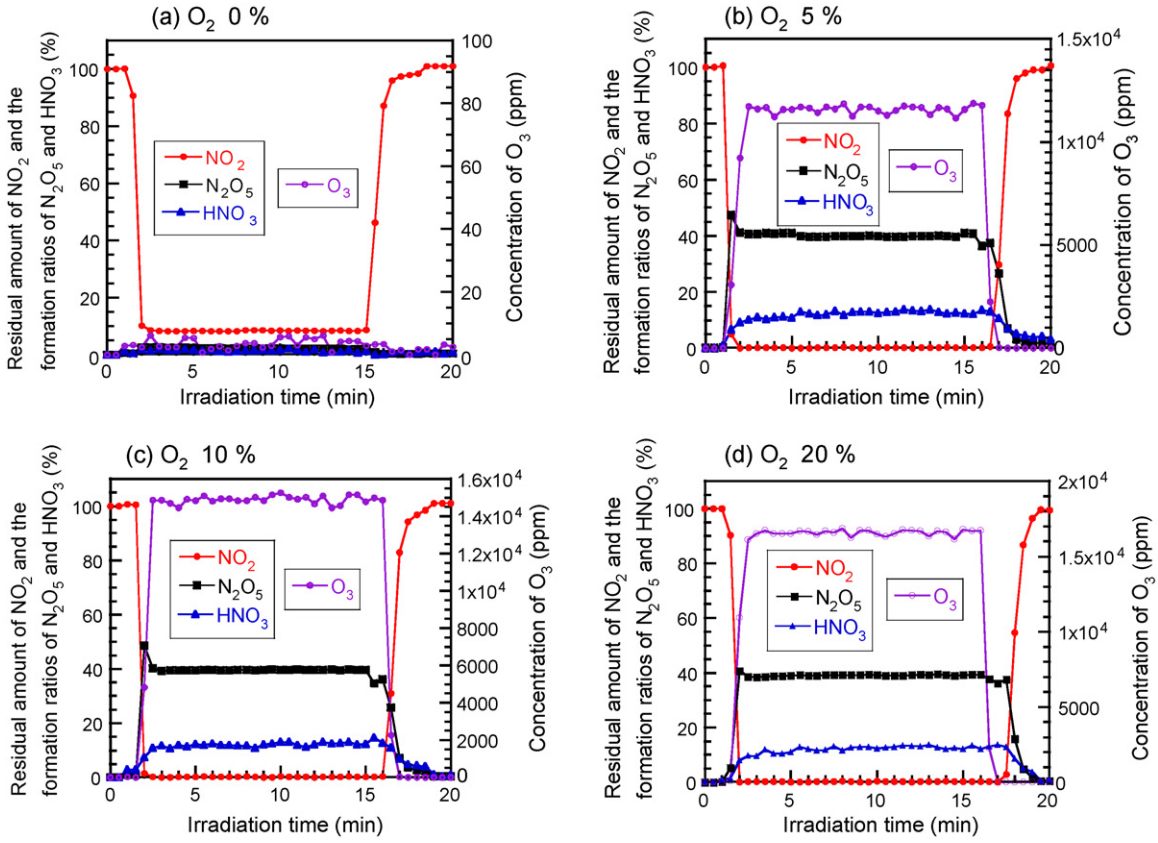

Fig. 8. Dependence of the residual amount of NO_2, the formation ratios of products, and the concentration of O_3 on the irradiation time in a flow system. Lamp was switched on at 1 min and off at 16 min. The initial NO_2 concentration was 200 ppm.

cult to efficiently decompose NO_2 in the flow system by using the low-power lamp. However, the flow system could be applied to the removal of NO_2, when the high-power lamp was used. Fig. 8a–d shows the dependence of residual amount of NO_2 and the formation ratios of NO_2, N_2O_5, and HNO_3 and concentration of O_3 on the irradiation time of lamp in the flow system in air (0, 5, 10, and 20% O_2), when 200 ppm of NO_2 was used. The Xe_2 lamp was switched on at 1 min and switched off at 16 min. In N_2 atmosphere, about 90% of NO_2 was dominantly converted to N_2 and O_2 at a steady state conditions. Small amounts of N_2O_5 and HNO_3 were also produced as minor products at low formation ratios of 2 and 1.5%, respectively. It should be noted that NO_2 can be completely converted after the lamp was switched on about 1 min in air (5–20% O_2). The formation ratios of N_2O_5 and HNO_3 were nearly constants at ~40 and ~12%, respectively, in this O_2 concentration range. On the basis of N balance, about ~92% of NO_2 is converted to N_2O_5 and HNO_3, and the rest of it is converted to N_2 and O_2 with the formation ratios of ~4 and ~8%, respectively. The concentration of O_3 increases to 12,000, 15,000, and 16,600 ppm with increasing the O_2 concentration from 5 to 20%. These results indicate that NO_2 can be removed efficiently in the flow system as N_2 and O_2 in N_2 and N_2O_5, HNO_3, N_2, and O_2 in air under 172-nm excimer lamp irradiation.

The maximum amount of NO_2, which can be removed in our flow system, was evaluated by changing the NO_2 concentration. Fig. 9 shows the dependence of the residual amount of NO_2 on the initial concentration of NO_2 in air (20% O_2). It was found that NO_2 can be removed in the 200–400 ppm range, whereas the residual amount of NO_2 slightly decreases from 70 to 60% with increasing the NO_2 concentration from ~500 to ~1000 ppm. In order to convert NO_2 to N_2O_5 and HNO_3, sufficient amounts of O_3 are necessary as discussed in Section 3.6. The main reason why the NO_2 cannot be removed more than 40% with increasing the NO_2 initial concentration from ~500 to ~1000 ppm is insufficient amounts of O_3 to convert all NO_2. The main products in the 200–400 ppm were N_2O_5 and HNO_3 and O_3, whereas they were N_2 and O_2 in the 500–1000 ppm range. Since the flow rate of our experiment was kept at 1 l/min, 16 μmol/min of NO_2 can be removed in our present system in air (20% O_2).

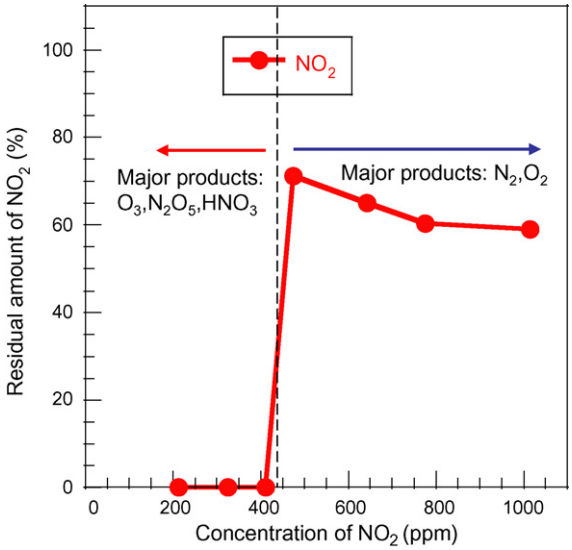

Fig. 9. Dependence of the residual amount of NO_2 on the initial concentration of NO_2 in a flow system in air (20% O_2).

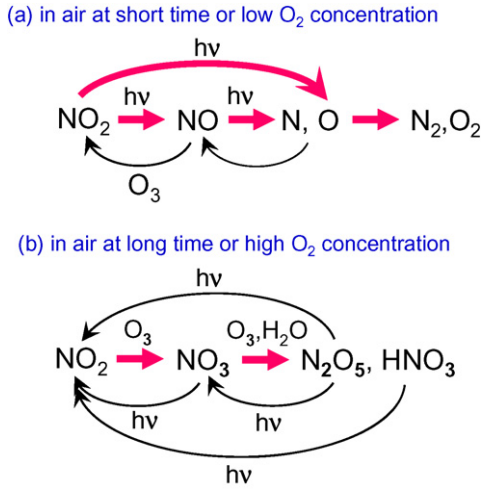

Fig. 10. Two models of major decomposition processes of NO_2 in O_2 under 172-nm irradiation.

3.6. The mechanism of NO_2 removal in air under 172-nm irradiation

The reaction mechanism of NO_2 in air is discussed from known photochemical and gas phase reactions [29–31]. There are two cases for the NO_2 removal process in air. The first case occurs at a short time or low O_2 concentrations (model (a) in Fig. 10), whereas the second case happens at a long time or high O_2 concentrations (model (b) in Fig. 10). The initial step is slow photolysis of NO_2 to N_2 and O_2 without the presence of O_3. In this step, O_3 is produced via famous VUV photolysis of O_2 followed by the three-body reaction:

$$O_2 + h\nu\,(172\,\text{nm}) \rightarrow O + O\,(4.6 \times 10^{-19}\,\text{cm}^2\,\text{molecule}^{-1}) \quad (18a)$$

$$O + O_2 + M \rightarrow O_3 + M\,(5.6 \times 10^{-34}\,\text{cm}^6\,\text{molecule}^{-2}\,\text{s}^{-1}\ \text{for M} = N_2) \quad (18b)$$

At short irradiation times, the concentrations of NO_2 and NO after photolysis of NO_2 are high, whereas the concentration of O_3 is low. Under these conditions, O_3 is completely consumed through the following processes:

$$NO_2 + h\nu\,(172\,\text{nm}) \rightarrow NO + O(^3P, {}^1D, {}^1S) \quad (16a)$$

$$NO + O_3 \rightarrow NO_2 + O_2\,(1.8 \times 10^{-14}\,\text{cm}^3\,\text{molecule}^{-1}\,\text{s}^{-1}) \quad (6)$$

These cyclic reactions, which are famous reactions as destruction of ozone layer in the upper atmosphere [1], occur significantly. In this case, concentrations of NO and O_3 are either zero or very low. In the second step, the concentration of O_3 becomes sufficiently high, so that extra O_3 is accumulated in the photolysis chamber. In such a case, O_3 concentration is higher than that required for (6) and the reaction of excess O_3 with NO_2 leading to N_2O_5 takes place:

$$NO_2 + O_3 \rightarrow NO_3 + O_2\,(3.5 \times 10^{-17}\,\text{cm}^3\,\text{molecule}^{-1}\,\text{s}^{-1}) \quad (19)$$

$$NO_2 + NO_3 + N_2 \rightarrow N_2O_5 + N_2\,(3.6 \times 10^{-30}\,\text{cm}^6\,\text{molecule}^{-2}\,\text{s}^{-1}) \quad (20)$$

In the photolysis chamber, there is a small amount of residual H_2O (~90 ppm), as observed OH peaks from residual H_2O in FTIR spectra. N_2O_5 has a high reactivity with H_2O leading to HNO_3:

$$N_2O_5 + H_2O \rightarrow 2HNO_3\,(2.5 \times 10^{-22}\,\text{cm}^3\,\text{molecule}^{-1}\,\text{s}^{-1}) \quad (21)$$

Thus, HNO_3 peaks arise from the result of reaction (21). Reaction (21) is an important reaction, because N_2O_5 can be easily removed as HNO_3 by the addition of H_2O. The following backward photolysis reactions must occur competitively under 172-nm irradiation:

$$N_2O_5 + h\nu\,(172\,\text{nm}) \rightarrow NO_3 + NO_2 \quad (22)$$

$$NO_3 + h\nu\,(172\,\text{nm}) \rightarrow NO_2 + O \quad (23)$$

$$HNO_3 + h\nu\,(172\,\text{nm}) \rightarrow NO_2 + OH \quad (24)$$

However, the conversion of NO_2 to N_2O_5, HNO_3, N_2, and O_2 occurs completely. This indicates that these reactions are suppressed completely because dark reactions occur between the photolysis chamber and the gas analysis chamber at high O_3 concentrations.

The reaction mechanism of NO_2 in air (5–20% O_2) in the flow system is expected to be similar to that of the second step, because excess amounts of O_3 were always present in the photolysis chamber. In such a condition, oxidation reactions of NO_2 leading N_2O_5 and subsequent reaction between N_2O_5 and H_2O leading HNO_3 become significant. This process occupies about 92% of the total conversion of NO_2 and the rest is the conversion to N_2 and O_2 via photolysis.

4. Conclusion

In summary, deNOx process by using 172-nm excimer lamp has been studied to develop a new photochemical removal process without using any catalysts. It was found that 200–400 ppm of NO_2 can be efficiently converted to N_2 and O_2 in N_2 and to N_2O_5 and HNO_3 in air in a flow system by using a high-power Xe_2 lamp (300 mW/cm^2). N_2O_5 can be easily converted to HNO_3 by the addition of H_2O, and N_2O_5 and HNO_3 can be easily trapped in water and several reduction processes of NO_3^- anions to N_2 in water have already been developed at normal temperatures and pressures. Therefore, by combination the present method with such processes, a new photochemical aftertreatment technique of NO_2 in N_2 and air without using any catalysts will be developed. In air, O_3 was used as a key material in this aftertreatment technique of NO_2. Since O_3 is a source gas of photochemical smog, its emission should also be suppressed. In our present flow system, it is possible to suppress O_3 concentration by monitoring and controlling O_3 concentration in the exhausted gases. Thus, O_3 emission will not be a great problem in our apparatus. Unfortunately, little information on products and their yields has been reported for 172-nm photolysis of NOx, O_2, and O_3. Therefore, such fundamental information is required for the improvement of the present photochemical process. In addition, for the practical application of photochemical process for NO_2 removal, effects of other emitting species such as SO_2, CO, CO_2, hydrocarbons, H_2O, and particulate matter, which are generally involved in the exhausted gases, must be examined.

Acknowledgements

This work was partly supported by JST-CREST and Joint Project of Chemical Synthesis Core Research Institutions. The authors thank Ushio Inc. for the use of a high power Xe_2 excimer lamp.

References

[1] D.J. Jacob, Introduction to Atmospheric Chemistry, Princeton University Press, New Jersey, 1999.
[2] Acid Rain: US Environmental Protection Agency, http://www.epa.gov/acidrain/.
[3] R.M. Heck, R.J. Farrauto, S.T. Gulati, Catalytic Air Pollution Control: Commercial Technology, Wiley–Interscience, Weinheim, 2002.
[4] N. Nejar, M. Makkee, M.J. Illán-Gómez, Catalytic removal of NOx and soot from diesel exhaust: oxidation behaviour of carbon materials used as model soot, Appl. Catal. B: Environ. 75 (2007) 11–16.

[5] J.R. Theis, E. Gulari, Estimating the temperatures of the precious metal sites on a lean NOx trap during oxidation reactions, Appl. Catal. B: Environ. 75 (2007) 39–51.
[6] X. Hu, J. Nicholas, J.J. Zhang, T.M. Linjewile, P. de Filippis, P.K. Agarwal, The destruction of N_2O in a pulsed corona discharge reactor, Fuel 81 (2002) 1259–1268.
[7] X. Hu, J.J. Zhanga, S. Mukhnahallipatna, J. Hamann, M.J. Biggs, P. Agarwal, Transformations and destruction of nitrogen oxides—NO, NO_2 and N_2O—in a pulsed corona discharge reactor, Fuel 82 (2003) 1675–1684.
[8] S. Yao, M. Okumoto, T. Yashima, J. Shimogami, K. Madokoro, E. Suzuki, Diesel particulate matter and NOx removals using a pulsed corona surface discharge, AICHE J. 50 (2004) 715–721.
[9] K. Onda, H. Kusunoki, K. Ito, H. Ibaraki, Numerical analysis of repetitive pulsed-discharge de-NOx process with ammonia injection, J. Appl. Phys. 95 (2004) 3928–3936.
[10] J. Vinogradov, B. Rivin, E. Sher, NOx reduction from compression ignition engines with DC corona discharge—an experimental study, Energy 32 (2007) 174–186.
[11] Z.H. Wang, J.H. Zhou, Y.Q. Zhu, Z.C. Wen, J.Z. Liu, K. Cen, Simultaneous removal of NOx, SO_2 and Hg in nitrogen flow in a narrow reactor by ozone injection: experimental results, Fuel Process. Technol. 88 (2007) 817–823.
[12] Y. Yankelevich, M. Wolf, R. Baksht, A. Pokryvailo, J. Vinogradov, B. Rivin, E. Sher, NOx diesel exhaust treatment using a pulsed corona discharge: the pulse repetition rate effect, Plasma Sources Sci. Technol. 16 (2007) 386–391.
[13] J.X. Yang, X.C. Chi, L.M. Dong, Effect of water on sulfur dioxide (SO_2) and nitrogen oxides (NOx) removal from flue gas in a direct current corona discharge reactor, J. Appl. Phys. 101 (2007) 103304 (5 pp.).
[14] M. Tsuji, T. Tanoue, K. Nakano, A. Tanaka, Y. Nishimura, Superior decomposition of N_2O into N_2 and O_2 in a fast discharge flow of N_2O/He or N_2O/Ar mixtures, Jpn. J. Appl. Phys. 39 (2000) L1330–L1333.
[15] M.A. Wójtowicz, F.P. Miknis, R.W. Grimes, W.W. Smith, M.A. Serio, Control of nitric oxide, nitrous oxide, and ammonia emissions using microwave plasmas, J. Hazard. Mater. 74 (2000) 81–89.
[16] M. Tsuji, T. Tanoue, J. Kumagae, K. Nakano, Decomposition of N_2O by microwave discharge of N_2O/He or N_2O/Ar mixtures, Jpn. J. Appl. Phys. 40 (2001) 7091–7097.
[17] M. Baeva, A. Pott, J. Uhlenbusch, Modelling of NOx removal by a pulsed microwave discharge, Plasma Sources Sci. Technol. 11 (2002) 135–141.
[18] M. Tsuji, J. Kumagae, K. Nakano, T. Tsuji, Decomposition of N_2O in a microwave-absorbent assisted discharge of N_2 at atmospheric pressure, Appl. Surf. Sci. 217 (2003) 134–148.
[19] M. Tsuji, K. Nakano, J. Kumagae, T. Matsuzaki, T. Tsuji, Decomposition of NO in a microwave-absorbent assisted discharge of N_2 at atmospheric pressure, Surf. Coat. Technol. 165 (2003) 296–308.
[20] J.W. Tang, T. Zhang, L. Ma, N. Li, Direct decomposition of NO activated by microwave discharge, Ind. Eng. Chem. Res. 42 (2003) 5993–5999.
[21] K. Krawczyk, K. Naperty, M. Drozdowski, Microwave reactor for nitrous oxide processing, J. Adv. Oxid. Technol. 9 (2006) 160–163.
[22] K. Krawczyk, M. Drozdowski, K. Naperty, Nitrous oxide processing by a combination of gliding and microwave discharges, Catal. Today 119 (2007) 239–242.
[23] J.L. Hueso, A.R. Gonzalez-Elipe, J. Cotrino, A. Caballero, Removal of NO in NO/N_2, $NO/N_2/O_2$, $NO/CH_4/N_2$, and $NO/CH_4/O_2/N_2$ systems by flowing microwave discharges, J. Phys. Chem. A 111 (2007) 1057–1065.
[24] M. Tsuji, J. Kumagae, T. Tsuji, T. Hamagami, N_2O removal in N_2 or air by ArF excimer laser photolysis at atmospheric pressure, J. Hazard. Mater. 108 (2004) 189–197.
[25] M. Tsuji, K. Noda, H. Sako, T. Hamagami, T. Tsuji, Efficient decomposition of NO_2 into N_2 and O_2 by 193 nm ArF laser in N_2 atmosphere, Chem. Lett. 34 (2005) 496–497.
[26] M. Tsuji, H. Sako, K. Noda, M. Senda, T. Hamagami, T. Tsuji, Efficient photochemical conversion of N_2O into N_2 and O_2 by 193 nm ArF excimer laser in N_2 or air at atmosphere pressure, Chem. Lett. 34 (2005) 812–813.
[27] M. Tsuji, H. Sako, M. Senda, K. Noda, T. Hamagami, M. Kawahara, T. Tsuji, Photochemical removal of N_2O in N_2 and air by ArF 193 nm excimer laser at atmospheric pressure over a wide N_2O concentration range, in: L.G. Mason (Ed.), Focus on Hazardous Materials Research, Nova Science Publishers, New York, 2007, pp. 143–163 (Chapter 4).
[28] M. Tsuji, M. Kawahara, M. Senda, K. Noda, Efficient conversion of NO_2 into N_2 and O_2 in N_2 and into N_2O_5 in air by 172-nm Xe_2 excimer lamp at atmospheric pressure, Chem. Lett. 36 (2007) 376–377.
[29] IUPAC Gas Kinetic Data Evaluation, Summary Table of Kinetic Data, June 2006 (http://www.iupac-kinetic.ch.cam.ac.uk).
[30] R. Atkinson, D.L. Baulch, R.A. Cox, R.F. Hampson Jr., J.A. Kerr, M.J. Rossi, J. Troe. J. Phys. Chem. Ref. Data 26 (1997) 1329–1499, Updated data were obtained from NIST Chemical Database on the Web, Public Beta Release 1.4, Standard Reference Database 17, Version 7.0 (http://kinetics.nist.gov/index.php).
[31] H. Okabe, Photochemisty of Small Molecules, John Wiley & Sons, New York, 1978.
[32] S.G. Lias, J.E. Bartmess, J.F. Liebman, J.L. Holmes, R.D. Levin, W.G. Mallard, J. Phys. Chem. Ref. Data 17 (Suppl. 1) (1988) 1, Updated Data were Obtained from NIST Standard Ref. Database, Number 69, June 2005 (http://webbook.nist.gov/chemistry).
[33] X. Wang, H. Li, Q. Ju, Q. Zhu, F. Kong, The vibrational quenching of NO ($v = 1–11$) by N_2O studied by time-resolved Fourier transform infrared emission spectroscopy, Chem. Phys. Lett. 208 (1993) 290–294.
[34] G. Hancock, M. Morrison, The 193 nm photolysis of NO_2: NO(v) vibrational distribution, $O(^1D)$ quantum yield and emission from vibrationally excited NO_2, Mol. Phys. 103 (2005) 1727–1733.
[35] I.J. Wysong, Vibrational energy transfer of NO ($X^2\Pi$, $v = 2$ and 1), J. Chem. Phys. 101 (1994) 2800–2810.